The effect of angle on shock wave boundary layer interaction

Author(s):
Qinghu, Zhang; Zhiwei, Zhu

Publication date:
2018-10-05

Permanent link:
https://doi.org/10.3929/ethz-b-000279169

THE EFFECT OF ANGLE ON SHOCK WAVE BOUNDARY LAYER INTERACTION

Zhang Qinghu[c], Zhu Zhiwei

Hypervelocity Aerodynamics Institute of China Aerodynamics Research and Development Center, Mianyang, China
[c]Corresponding author; Email: zhang_qinghu@163.com

KEYWORDS:
Main subjects: shock wave/boundary layer interaction
Fluid: hypersonic flow
Visualization method(s): Planar Laser Scattering (PLS)

ABSTRACT: *The incident shock interaction with the hypersonic laminar and forced turbulent boundary layer is visualized by the planar laser scattering technique. The average spatial features are obtained by two-point spatial correlation analysis. The effect of three angles on shock wave/boundary layer interaction is investigated. The results show that the boundary layer has been greatly influenced by the incident shock. Both the laminar and turbulent inflow, the boundary layer thickness has an abrupt decrease at the interaction region. In laminar inflow, the boundary layer transition rapidly takes place due to the incident shock. The greater angle, the bigger boundary layer thickness downstream the incident shock. With the stronger incident angles, the structure angle of the vortices at this position is smaller. In turbulent inflow, the thickness downstream the shock is less than that of inflow. Increasing incident angle has no obviously effect on the structure angles.*

1 Introduction

Shock wave/boundary layer interaction (SWBLI) is a widespread phenomenon at supersonic / hypersonic flow. It involves the Mach number, inflow boundary layer characteristics, incident shock angle and the flow geometry shape and can be a critical factor in determining the performance of a vehicle or a propulsion system [1].Owing to the importance in fundamental research and engineering application, it has been the subject of experimental and computational research for decades [2]. To understand the flow mechanism, SWBLI has been investigated from a variety of techniques, among them, the flow visualization is an effective method and has been widely used.

With the development the experimental technique, especially the laser technique, more and more studies of the SWBLI has focused on the fine structures and unsteadiness of the shock. Bookey [3] experimentally investigated a 12º reflected shock interaction using the Filtered Rayleigh Scattering (FRS), surface pressure distributions and surface flow visualizations. Humble [4] investigated an incident shock wave/turbulent boundary layer interaction at Mach 2.1 using particle image velocimetry (PIV). The results showed that the interaction exhibits a multi-layered structure, characterized by a relatively high-velocity outer region and low-velocity inner region. Smits [5] reviewed the basic research in hypersonic turbulent flows, including free shear layers, boundary layers, internal flows and shock-wave boundary layer interactions.

Planar Laser Scattering (PLS) is a flow imaging technique [6-8] and has been widely used in supersonic and hypersonic flow visualization. Using the PLS, Bueno [6] studied the time-dependent structure of shock-induced turbulent separation by the SWBLI. In this paper, the effect of angle on incident shock wave//boundary layer interaction is visualized and investigated.

2 Experimental setup

2.1 Flow facility

The experiments were conducted in the Φ 0.3 hypersonic blow-down wind tunnel of China Aerodynamics Research and Development Center (CARDC). The gas source is nitrogen. The total temperature is 288 K and the total pressure is 0.2 MPa. The experimental parameters are given in Table 1. The testing model for the incident shock wave boundary layer interaction is a flat-plate and a wedge fixed in the wind tunnel, as shown in Figure 1. The incident shock is producing by the wedge, the angle of which is adjustable. The length of the wedge is 200 mm and the width is 160 mm. The flat-plate dimensions are 300 mm in length and 200 mm in width, the middle flow of the plate can be seen as two-dimensional shock boundary layer interaction.

Table 1. Experimental parameters

Ma_∞	T_0 (K)	P_o (MPa)	Re (m^{-1})
5	288	0.2	6.2×10^6

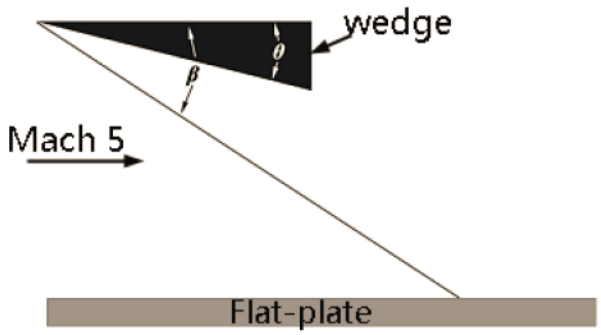

Fig. 1. The incident shock wave boundary layer interaction

2.2 Planar laser scattering

The flow was visualized with Planar Laser Scattering (PLS) where the scattering medium was condensed CO_2 fog. Poggie [7] and Hyungrok [8] have demonstrated the general use of this diagnostic technique for supersonic flows flows expanded through the converging/diverging nozzle. The setup for PLS imaging is composed of a dual-cavity Nd:YAG laser (by Beamtech Optronics), a particle generator, an interline transfer double-exposure CCD camera, a synchronizer and a computer. The laser with 500 mJ pulsed energy at the wavelength of 532 nm and 8 ns pulse duration is used as a light source. The laser beam is transformed into a uniform light sheet with the thickness less than 0.5 mm by a set of cylindrical lens. The flow is imaged using an interline transfer CCD camera (by Imperx) with the resolution of 4.8k×3.2k pixels.

3 Results and discussion

3.1 Laminar inflow

Figure 2 shows the images of incident shock wave interacting with the plane boundary layer. Herein, the angles of the wedge are 20° 、25° and 30, respectively, and the corresponding angles of the incident shock are 30°, 35.5°and 42°. The bottom of the images is the flat-plate and the origin x=0 is

located at the leading edge of the flat-plate. According to the flow organization of the interaction [1], the incident shock and the reattachment shock (marked as S) are clearly identified in Fig2. However, the reflected shock is not clearly identified. The reason might be PLS cannot clearly visualize the weakly waves. In Fig.2a, it can be seen than the incoming boundary layer is a thin layer with increasing thickness, which is laminar boundary layer. There are bulge structures due to the incident shock, which indicates that the boundary layer transition begin to take place. For comparison purpose, Figure 3 presents the flat-plate boundary layer without the shock at the same conditions. In Fig.3, the boundary layer at upstream of approximately x=240 mm is laminar and after that there are traveling structures marked as A. Compare with the Fig.3, the boundary layer transition occurs early due to the perturbation of the shock. At the same time, the boundary layer has an abrupt increase just upstream the incident shock and it has an abrupt decrease along the incident shock direction in Fig.2a. Subsequently, the boundary layer transforms into a series of vortices downstream the shock. At the beginning, the size of vortices is small, and then it becomes bigger in the downstream. It can be seen that the boundary layer has been greatly changed by the incident shock. The premature boundary layer transition is brought by the incident shock and the size and conformation of the boundary layer are influenced by the shock.

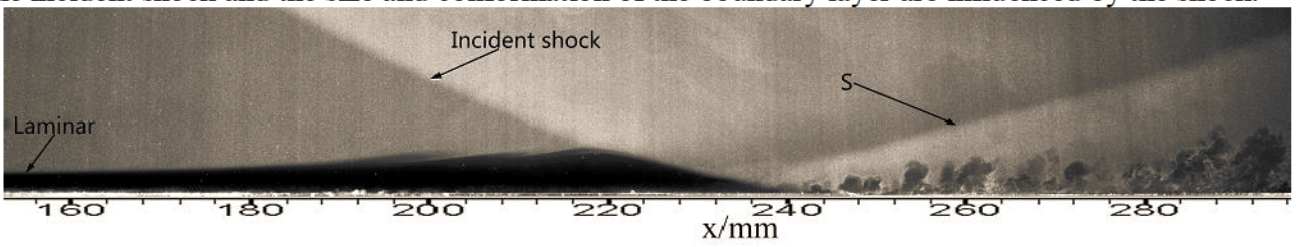

(a) incident shock angle 30°

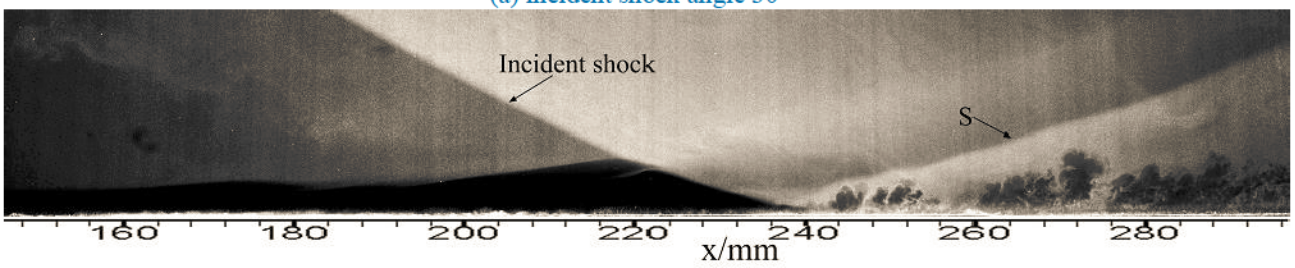

(b) incident shock angle 35°

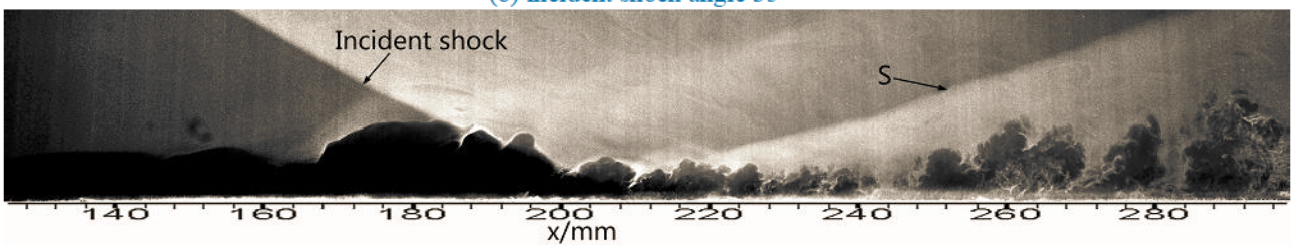

(c) incident shock angle 42°

Fig. 2. Images of shock wave/boundary layer interaction with different incident angles

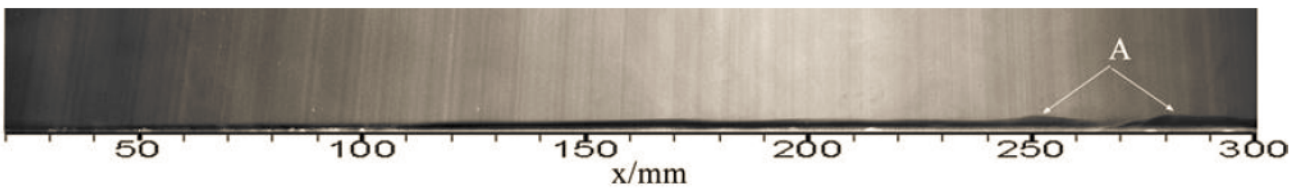

Fig. 3. Image of flat-plate boundary layer at Mach 5

In Fig.2b, it has the same flow structure with that in Fig.2a, except the boundary layer thickness. In Fig.2c, the boundary layer transition occurs earlier upstream and the boundary layer thickness increased with the stronger incident shock. By processing the PLS images, the average boundary layer information can be acquired. Figure 4 shows the average boundary layer thickness of laminar inflow SWBI, which is the mean from 200 images. The X coordinate is the same as the Fig.2 and h coordinate is height of the boundary layer. Herein, the boundary layer thickness is obtained by the PLS images, which is not the common velocity boundary layer. It can be seen that the variation of the boundary layer thickness is very similar. The boundary layer increases nearly linear upstream of the incident shock; it has an abrupt decrease in thickness at the interaction region; it increase along the plate and the growth rate is slowing in downstream of the shock. With the increasing angle of the shock, the boundary thickness is also increase. With the bigger angle, the growth rate is faster.

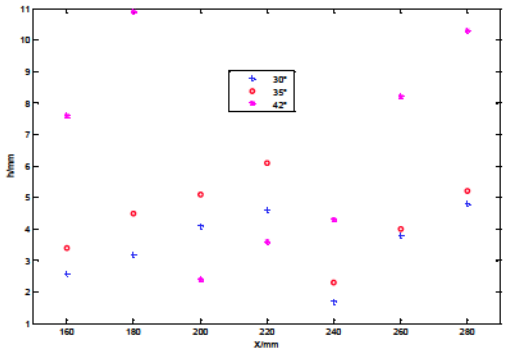

Fig. 4. The average boundary layer thickness of laminar inflow SWBLI

To quantify the average spatial features of the vortex structures, two-point spatial correlation functions are evaluated statistically according to

$$R(i,j)=\frac{\sum_{n=1}^{N}(I_n(i,j)-\overline{I}(i,j))(I_n(i_0,j_0)-\overline{I}(i_0,j_0)}{\sqrt{\sum_{n=1}^{N}(I_n(i,j)-\overline{I}(i,j))^2\sum_{n=1}^{N}(I_n(i_0,j_0)-\overline{I}(i_0,j_0))^2}} \quad (1)$$

where I_n is the gray value of the nth sample image, i and j are pixels coordinates, 0 denotes a reference coordinate, and the over bar represents the mean value. Figure 5 presents the structure angles at $0.8\,\delta_{local}$ of laminar inflow SWBI, which are computed from an ensemble of 200 images. The X coordinate is the same as the Fig.2 and α coordinate is structure angle. Here, δ_{local} is the local boundary layer thickness from the PLS images. The structure angles are calculated from the 0.5 contour curves from the two-point spatial correlation results. For more calculated detail, see reference [9]. It can be seen that the structure angles of the three incident angles becoming small in downstream area. The structure angle of the three incident angles at x=280 mm are lower than 40°, which are close to the 36.1°of the Mach 4.9 plane turbulent boundary layer at $0.8\,\delta_{local}$ in reference [9]. With the stronger incident angles, the structure angle at the same x coordinates is smaller.

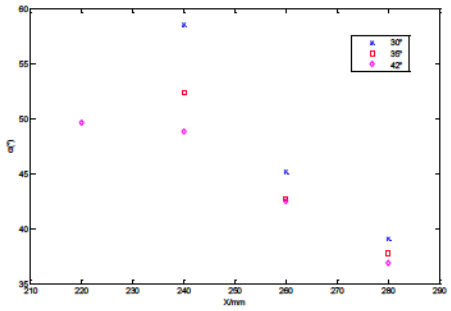

Fig. 5. Structure angles at 0.8 δ_{local} of laminar inflow SWBLI

3.2 Turbulent inflow

In order to obtain the turbulent boundary layer, the micro-ramps with 4 mm height is placed at the x=80mm. The origin x=0 is located at the leading edge of the flat-plate. Figure 67 presents the images of incident shock wave interacting with the forced turbulent boundary layer. The angles of the incident shock are 30°, 35.5°and 42°. The shock (marked as S) is the reattachment shock. In Fig.6 the inflow boundary layer exhibits the large-scale structures and is the turbulent boundary layer. The boundary layer thickness is fairly decreased at the shock interaction zone and it has abrupt decrease downstream the shock. The boundary layer thickness is less than the corresponding shock position and increase along the downstream direction. With the stronger incident shock, the boundary layer downstream the shock becomes more intermittent.

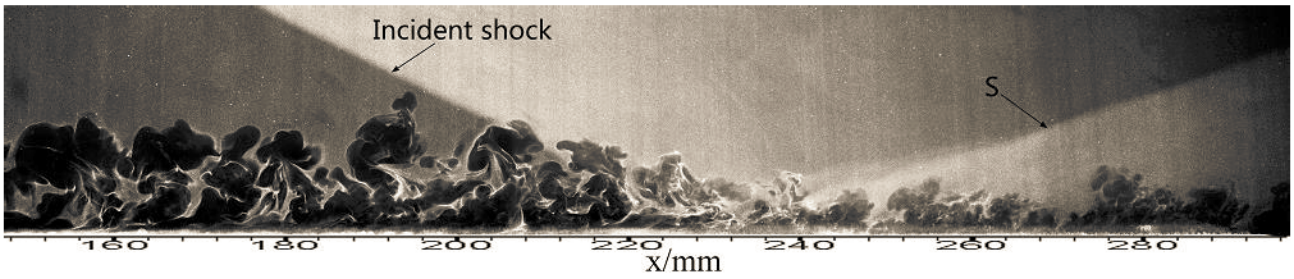

(a) incident shock angle 30°

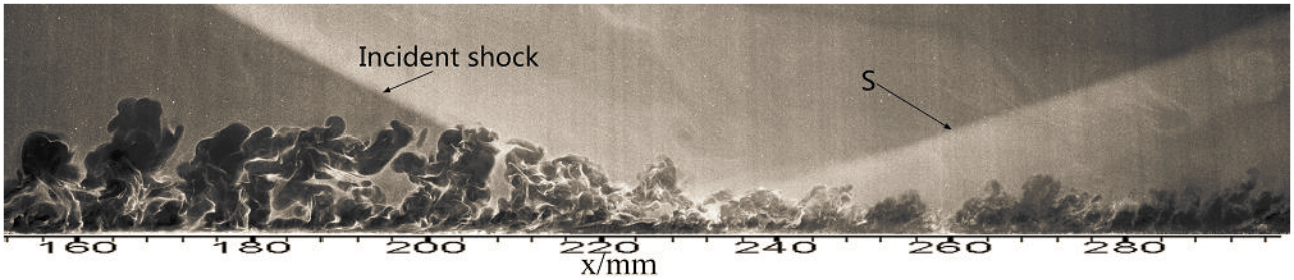

(b) incident shock angle 35°

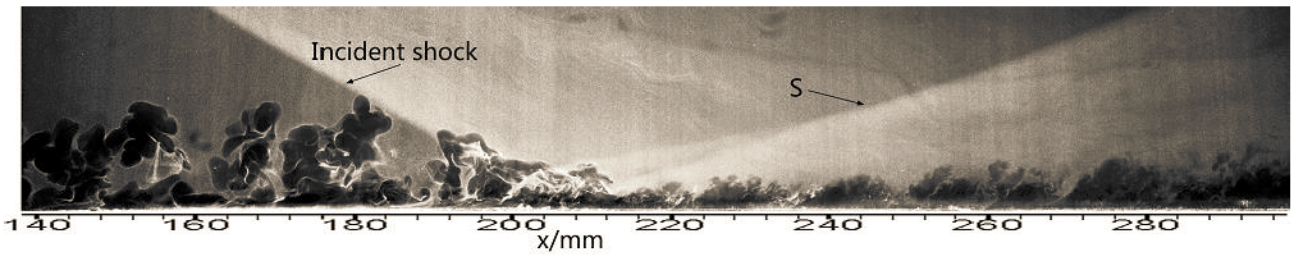

(c) incident shock angle 42°

Fig. 6. Images of shock wave/forced turbulent boundary layer interaction with different incident angles

Figure 7 shows the average boundary layer thickness of laminar inflow SWBI, which is the mean from 256 images. The X coordinate is the same as the Fig.6 and h coordinate is height of the boundary layer. It can be seen that the turbulent boundary layer thickness are almost constant upstream of the incident shock. The increasing angle of the incident shock is almost no effect on the boundary layer thickness upstream of the shock. It has an abrupt decrease in thickness at the interaction region. The bigger angle, the more decrease. Downstream the shock, it increases slowly and it is lower than that of the turbulent inflow. Figure 8 presents the structure angles at $0.8\,\delta_{local}$ of laminar inflow SWBI, which are computed from an ensemble of 200 images. The parameters are the same as those in Fig.5. It can be seen that the structure angles in upstream are about 38° and are not affected by the incident shock. Downstream of the shock, they are slight smaller than that of the inflow just downstream the shock. However, they are very close to that of the inflow. Increasing incident angle has no obvious effect on the structure angles.

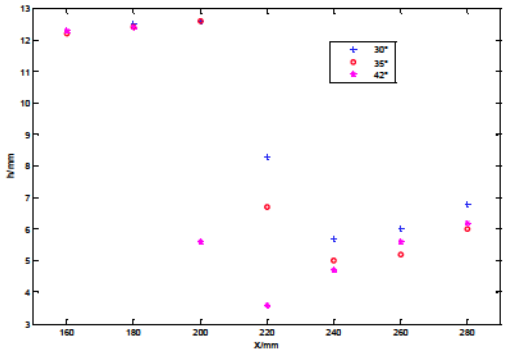

Fig. 7. The average boundary layer thickness of turbulent inflow SWBLI

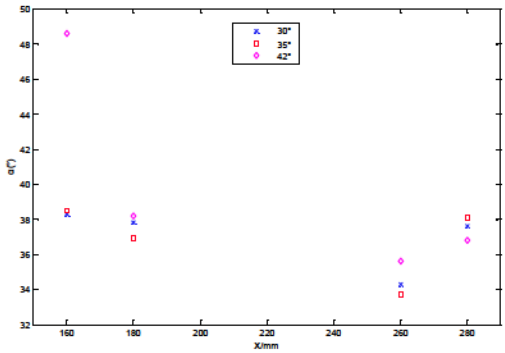

Fig. 8. Structure angles at 0.8 δ_{local} of turbulent inflow SWBLI

4 Conclusions

The incident shock interaction with the hypersonic laminar and forced turbulent boundary layer is visualized by the planar laser scattering technique. The high resolution flow images and average spatial features are obtained. It reveals the fine structures of shock wave/boundary layer interaction. The effect of three angles on shock wave/boundary layer interaction is investigated. The results show that the boundary layer has been greatly influenced by the incident shock. Both the laminar and turbulent inflow, the boundary layer thickness has an abrupt decrease at the interaction region. In laminar inflow, the boundary layer transition rapidly takes place due to the incident shock. The greater angle, the bigger boundary layer thickness downstream the incident shock. With the stronger incident angles, the structure angle of the vortices at the position is smaller. In turbulent inflow, the thickness downstream the shock is less than that of inflow. Increasing incident angle has no obviously effect on the structure angles.

Acknowledgements This study was supported by the National Natural Science Foundation of China (Grant no. 11502280).

References

[1] Babinsky H and Harvey J K. *Shock wave-boundary-layer interactions*, 1st edition, Cambridge, 2011.

[2] Gaitonde DV. Progress in shock wave/boundary layer interactions. *43rd AIAA Fluid Dynamics Conference,* San Diego, AIAA 2013-2607, pp 1-24, 2013.

[3] Bookey P and Wyckham C. New experimental data of STBLI at DNS/LES accessible reynolds number, *43rd AIAA Aerospace Sciences Meeting and Exhibit*, Reno, AIAA 2005-309, pp 1-18, 2005

[4] Humble R A, Scarano F and Oudheusden B W, Unsteady aspects of an incident shock wave/turbulent boundary layer interaction, *J. Fluid Mech.*, Vol. 635, pp 47-74,2009.

[5] Smits AJ, Martin PM and Girimaji S. Current status of basic research in hypersonic turbulence, *47th Aerospace Science Meeting*, Orlando FL, AIAA-2009-151,pp 1-32, 2009.

[6] Bueno PC, Ganapathisubramani B, Clemens BT and Dolling DS. Cinematographic Planar Imaging of a Mach 2 Shock Wave / Turbulent Boundary Layer Interaction. 43rd AIAA Aerospace Sciences Meeting and Exhibit, Reno, AIAA 2005-441, 99 1-19, 2005.

[7] Poggie J, Erland PJ, Smits AJ and Miles R B. Quantitative visualization of compressible turbulent shear flows using condensate-enhanced Rayleigh scattering. *Exp Fluids*, Vol. 37, pp 438–454, 2004.

[8] Hyungrok D, Seong-kyun I, Godfrey M and Mark AC. Visualizing supersonic inlet duct unstart using planar laser Rayleigh scattering. *Exp Fluids,* Vol. 50, pp 1654–1657, 2011.

[9] Humble RA, Peltier SJ and Bowersox RDW. Visualization of the structural response of a hypersonic turbulent boundary layer to convex curvature. *Physics of Fluid,* Vol. 24, pp 106103, 2012.

[10]